

Physical characteristics of $\text{Pb}_{1-x}\text{A}_x\text{Se}$ (A=Fe, Mn, V) for spintronic applications

M. Arshad^a, M. Yaseen^{a,*}, S. A. Aldaghfag^b, S. Saleem^a, M. Ishfaq^a, M. Nazar^a,
E. Yousef^{c,d}, H. H. Hegazy^{c,d}

^a*Spin-Optoelectronics and Ferro-Thermoelectric (SOFT) Materials and Devices Laboratory, Department of Physics, University of Agriculture Faisalabad 38040, Pakistan*

^b*Department of Physics, College of Sciences, Princess Nourah bint Abdulrahman University, P. O. Box 84428, Riyadh 11671, Saudi Arabia*

^c*Research Center for Advanced Materials Science (RCAMS), King Khalid University, Abha 61413, P. O. Box 9004, Saudi Arabia.*

^d*Physics Dep., Faculty of Science, King Khalid University, P. O. Box 9004, Abha, Saudi Arabia.*

The full-potential linearized-augmented plane wave (FP-LAPW) technique within Density functional theory (DFT) is used to compute the electronic, optical, and magnetic features of Fe, Mn and V doped binary compound PbSe. The effect of doping on energy band gap (E_g) and density of states (DOS) has been studied in detail. The computational results of DOS and band structure (BS) have confirmed that PbSe compound exhibit half-metallic ferromagnetic (HMF) nature. The E_g of PbSe binary compound is 0.16 eV which is enhanced up to 0.35, 0.23 and 0.54 eV after doping of Fe, Mn and V, respectively. Moreover, optical properties of Fe, Mn and V doped PbSe has been also studied in term of dielectric constants, absorption coefficient $\alpha(\omega)$, extinction coefficient $k(\omega)$, refractive index $n(\omega)$ and reflectivity $R(\omega)$. The magnetic properties are calculated and it is computed that $\text{Pb}_{0.75}\text{Mn}_{0.25}\text{Se}$ has greater magnetic moment (μ_B) as compared to $\text{Pb}_{0.75}\text{Fe}_{0.25}\text{Se}$, and $\text{Pb}_{0.75}\text{V}_{0.25}\text{Se}$. All the results revealed the appropriateness of $\text{Pb}_{1-x}\text{A}_x\text{Se}$ (A=Fe, Mn, V) materials for spinelectronics and optical gadgets.

(Received May 18, 2022; Accepted August 22, 2022)

Keywords: Transition metals, Binary compounds, Spintronics, Half metallic

1. Introduction

Dilute magnetic semiconductors (DMS) have been widely studied in the recent two decades due to their various application, including spintronics, spin FET and nano size integrated magnetic memory. [1, 2]. By substituting *4f* rare earth metals or *3d* magnetic transition metals (TMs) in semiconductors lattices, DMS are established. Furthermore, the suitable materials for spintronics are half metals which can be used as hybrids among metals and semiconductors [3-5]. The hypothesis of half metallic ferromagnetic (HMF) was introduced in 1983 by computing the electronic BS of Heusler alloys such as PtMnSb and NiMnSb, [6]. These materials are very important owing to their usage in tunnel junctions [7], effectual magnetic sensors [8], and magnetic devices [9, 10].

Lead selenide have been studied widely over past many years due to their different usages in electronic gadgets and thermoelectric energy convertors [11]. The compound has attracted researchers because of its ferroelectric behavior, electronic band gap and phase transitions. Moreover, the compound has shown exceptional optical and transport properties [12]. The group IV- VI binary compounds such as PbTe, PbS, PbSe, and their alloys PbEuTe, PbSnSe, PbSrSe, PbSnTe are being used in diode lasers, thermo-photovoltaic devices, and as long wavelength imaging devices [13]. Etgar et al. studied the magnetic and optical behavior of PbSe nanoparticles

* Corresponding author: myaseen_taha@yahoo.com
<https://doi.org/10.15251/CL.2022.198.553>

and found the compound suitable for various applications such as cancer cells detection, bio sensing, and spintronics [14]. Haq et al. probed the optoelectronic features of monolayer PbSe by first principle and calculated its effectiveness for photovoltaic and optoelectronic devices [15]. Gai et al. calculated the electronic properties of PbSe and stated that theoretical computations are approximated with experimental results [16].

In this research, we investigated the magnetic, electronic, and optical properties of transition metal (Fe, Mn and V) doped PbSe binary compound. The results of electronic properties showed the half metallic behavior of this doped compound. There is no previous research on Fe, V, and Mn doped PbSe compound which stimulate us to study its properties in details. The computed results are helpful to use this material in different fields like spintronics and optoelectronics.

2. Method of calculation

Density functional theory [17] is employed for magnetic, optical, and electronic calculations of Fe, Mn and V doped PbSe. The unit cell of the crystal contains two parts in FP-LAPW approach: muffin-tin region and interstitial region. The wave function and potential are extended outside the atomic sphere on plane wave basis and inside the atomic sphere on spherical harmonic basis [18, 19]. The equation for potential in both regions is written as:

$$V(r) = \begin{cases} \sum_{LM} V_{LM}(r)Y_{LM}(\hat{r}) & \text{inside sphere} \\ \sum_K V_K e^{iK.r} & \text{outside sphere} \end{cases} \quad (1)$$

All constraints can be identified in Hamiltonian of multiple body exchange correlation [20]. The 33-k points sampling is used to make grid of 1000 Monkhorst-pack meshes. The G_{\max} (Gaussian factor) for atomic radii conversion is taken as 14. Inside the muffin tin (MT) sphere, the angular momentum is expanded up to the $l_{\max}=10$. The muffin-tin radius (RMT) values are taken 2.2 for the Pb atom and the 2 Bohr for the Se atom. The binary compounds are made of two different elements and have an ideal cubic structure modeled in the Fm3m space group [21]. The structure of cubic unit cell of PbSe consists of unit formula and its Wyckoff-positions of the atoms are: Pb (0, 0, 0) and Se (0.25, 0.25, 0.25). Within GGA approximation, the value of lattice parameter $a=6.23\text{\AA}$ for PbSe was reported by using FP-LAPW method [22]. The electronic configuration for Pb, Se, Fe, Mn and V are [Xe] $4f^{14}5d^{10}6s^26p^2$, [Ar] $3d^{10}4s^24p^4$, [Ar] $3d^64s^2$, [Ar] $3d^54s^2$, and [Ar] $3d^34s^2$, respectively.

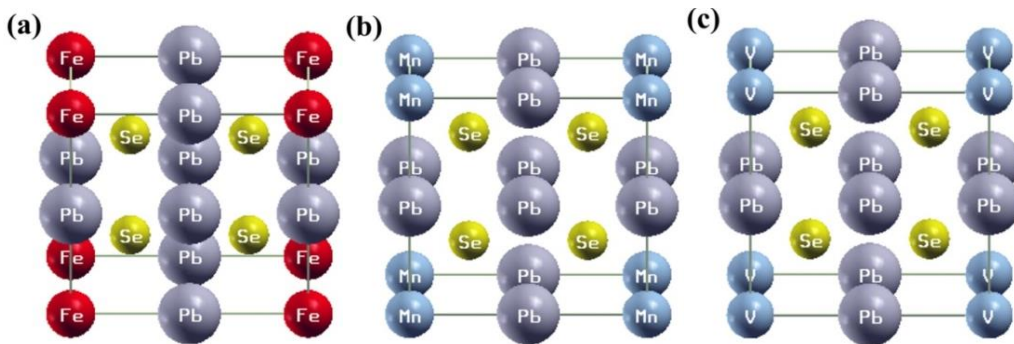
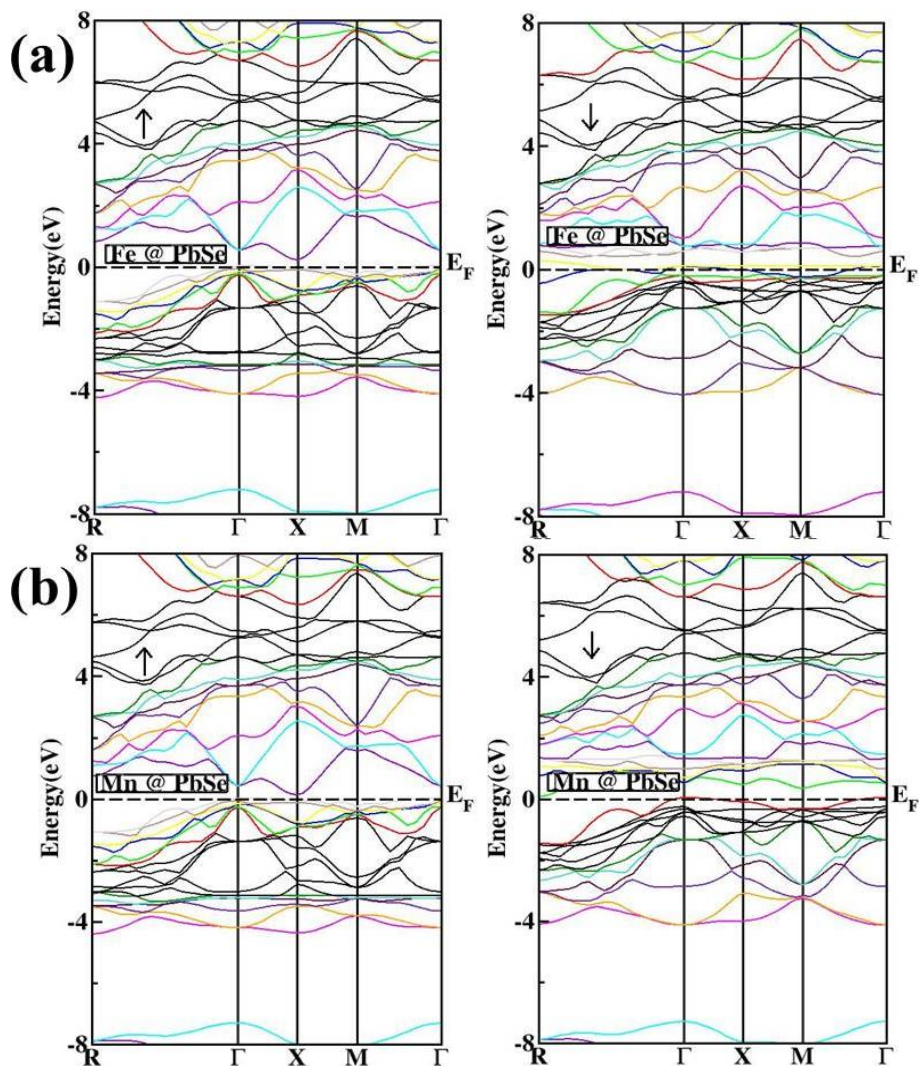


Fig. 1. Geometrical Structures for $x = 25\%$ (a) $Pb_{1-x}Fe_xSe$ (b) $Pb_{1-x}Mn_xSe$ (c) $Pb_{1-x}V_xSe$ compounds.

3. Results and discussions

3.1. Band Structures

Electronic characteristics based on band gap, TDOS and PDOS for Fe, Mn and V doped PbSe compounds are illustrated in the Fig. 1. The HM nature of the Fe, Mn and V doped PbSe have been shown in both spin version, correspondingly. The pure PbSe have shown direct energy gap in first Brillouin zone at the L-point having value of 0.16 eV [23], but the Fe, Mn and V doped PbSe have indirect band gap with half metallic nature. The calculated values of energy band gap of $\text{Pb}_{0.75}\text{Fe}_{0.25}\text{Se}$, $\text{Pb}_{0.75}\text{Mn}_{0.25}\text{Se}$ and $\text{Pb}_{0.75}\text{V}_{0.25}\text{Se}$ are 0.35, 0.23 and 0.54 eV, respectively (see Fig. 1 (a, b & c)). The V doped PbSe have large energy band gap as compared to the Fe, and Mn doped PbSe. Also, the value of energy band gap has been increased after doping with TM.



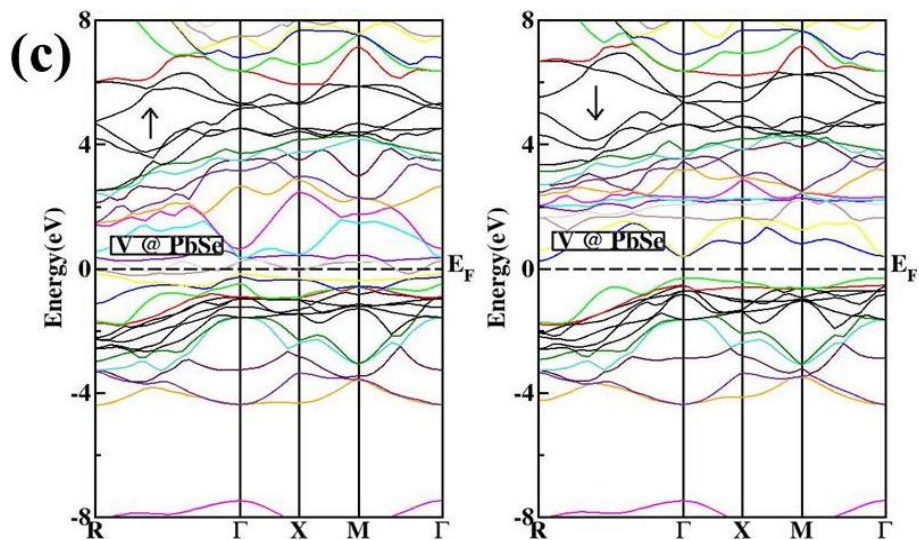


Fig. 2. Spin-polarized energy band plots for $x=25\%$ (a) $Pb_{1-x}Fe_xSe$ (b) $Pb_{1-x}Mn_xSe$ (c) $Pb_{1-x}V_xSe$.

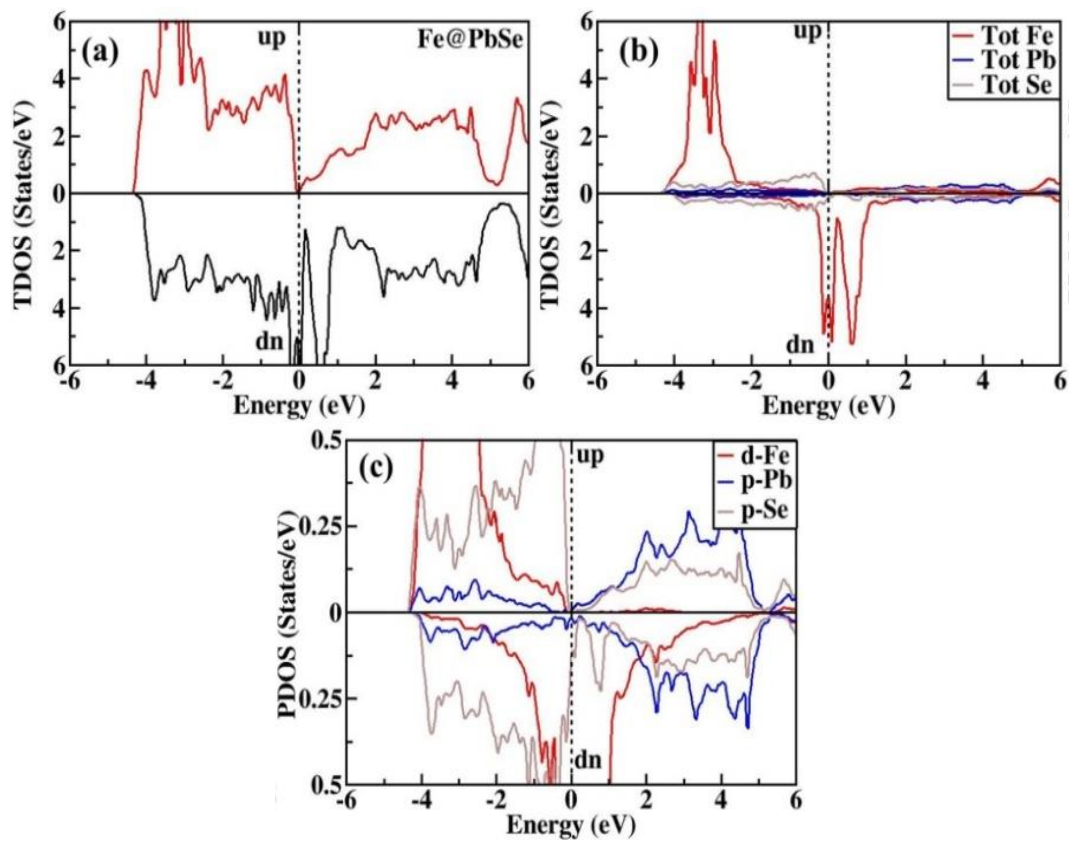


Fig. 3. Spin-Polarized (a) TDOS Fe doped PbSe (b) TDOS elements (c) and PDOS.

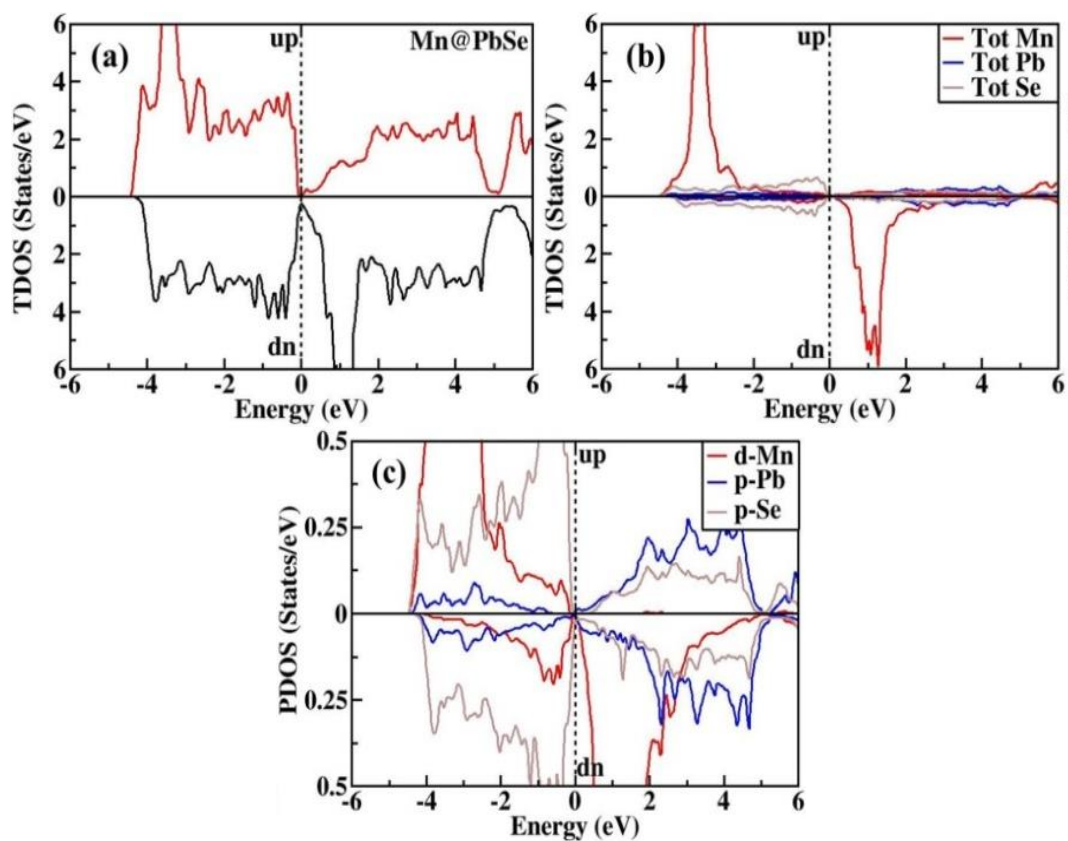


Fig. 4 Spin-Polarized (a) TDOS Mn doped PbSe (b) TDOS elements (c) and PDOS.

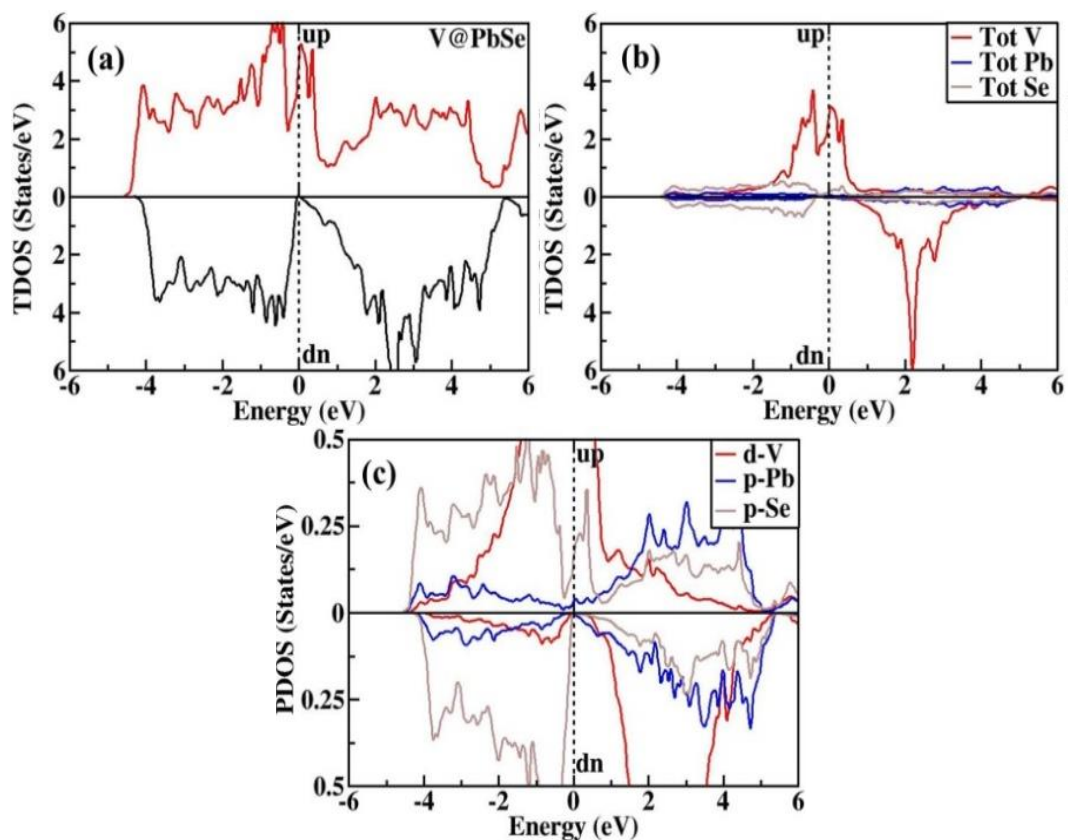


Fig. 5 Spin-Polarized (a) TDOS V doped PbSe (b) TDOS elements (c) and PDOS.

The characteristics of the electronic structures is further investigated from TDOS and the PDOS of Fe, Mn and V doped PbSe. Total and the partial DOS curves are shown in the Fig (2, 3 and 4). The Fe-*d*, Mn-*d*, and V-*d*, coincide with Fermi level and the contribution of these states is more than *s* and *p* states of Pb_{0.75}Fe_{0.25}Se, Pb_{0.75}Mn_{0.25}Se and Pb_{0.75}V_{0.25}Se compounds. The participation of Pb-*p*, and Se-*p* is greater as compared to Pb-*s* and Se-*d* orbitals which is shown in PDOS plots. It can be seen from the graphs that Pb_{0.75}Fe_{0.25}Se, Pb_{0.75}Mn_{0.25}Se and Pb_{0.75}V_{0.25}Se shows HMF nature. The variety of energy band gaps also indicates the applications of these compounds in spintronics devices like memory storage devices such as hard disk [24].

3.2. Magnetic properties

The observed magnetic moment of the Fe, Mn and V doped PbSe is summarized in the Table1. The interstitial magnetic moment (M_{int}) is 0.14088, 0.32354 and 0.50458 for the Pb_{0.75}Fe_{0.25}Se, Pb_{0.75}Mn_{0.25}Se and Pb_{0.75}V_{0.25}Se compounds, respectively. Total magnetic moments (M_{Tot}) of Pb_{0.75}Fe_{0.25}Se, Pb_{0.75}Mn_{0.25}Se and Pb_{0.75}V_{0.25}Se compounds are computed as 3.94233 μ_B , 4.99108 μ_B and 2.91084 μ_B respectively. The magnetic moment of Fe, Mn and V are 3.46630, 4.50630 and 2.79993, respectively. The value of Mn is greater as compared to Fe and V. All the results revealed that Fe, Mn and V doped PbSe compounds are appropriate for the spintronics devices. The magnetic moment can be calculated from edge splitting of the valence band ($\Delta E_V = E_V^\downarrow - E_V^\uparrow$) and conduction band ($\Delta E_C = E_C^\downarrow - E_C^\uparrow$) by using the following written equations:

$$N_o\alpha = \frac{\Delta E_C}{x\langle S \rangle} \quad (2)$$

$$N_o\beta = \frac{\Delta E_V}{x\langle S \rangle} \quad (3)$$

Where *x* represent concentration of the TM (Transition Metals) ion and $\langle S \rangle = \langle M \rangle / 2$, here $\langle M \rangle$ signifies M_{Tot} of the all particles in unit cell. The strong hybridizations among crystal fields splits the level of the unfilled 3-*d* states for Fe, Mn and V which confirmed ferromagnetic behaviors. It also causes in the reduction of the values of magnetic moments which contributes into PbSe and the interstitial sites.

Table 1. The calculated interstitial and atom resolved (Fe, Mn, V, Pb, Se) and the total magnetic moment of the Fe, Mn and V doped PbSe.

	Pb _{0.75} Fe _{0.25} Se	Pb _{0.75} Mn _{0.25} Se	Pb _{0.75} V _{0.25} Se
Interstitial	0.14088	0.32354	0.50458
Fe	3.46630	—	—
Mn	—	4.50630	—
V	—	—	2.79993
Pb	0.00913	0.02107	0.04903
Se	0.08356	0.03528	-0.11447
Total	3.94233	4.99108	2.91084

3.2. Optical properties

The optical features of Fe, V and Mn doped PbSe are investigated under the effect of electromagnetic field. These properties take place among the occupied and un-occupied states because of electric field of the photons. Therefore, with the help of dielectric function, optical features of any material can be deduced.

$$\varepsilon(\omega) = \varepsilon_1(\omega) + i\varepsilon_2 \quad (4)$$

The $\varepsilon_1(\omega)$ and $\varepsilon_2(\omega)$ of the $\varepsilon(\omega)$ are measured by Kramers-Kronig transformation. The curves in $\varepsilon_2(\omega)$ of dielectric constant are linked to different inter-band and the intra-band transitions in first BZ. The other optical parameters like $\alpha(\omega)$, $\sigma(\omega)$, $R(\omega)$, $K(\omega)$ and $n(\omega)$ are attained basically from the both $\varepsilon_1(\omega)$, and $i\varepsilon_2(\omega)$ parts [25].

The $\varepsilon_2(\omega)$ can be deduced from electronic BS using the relation:

$$\varepsilon_2(\omega) = \frac{e^2\hbar}{\pi m^2 \omega^2} \sum_{vc} \int |n, n'(k, q)|^2 [\omega n, n'(k) - \omega] d^3k \quad (5)$$

The $\varepsilon_1(\omega)$ can be computed from $\varepsilon_2(\omega)$ from the relation:

$$\varepsilon_1(\omega) = 1 + \frac{2}{\pi} p \int_0^\theta \frac{\omega' \varepsilon_2(\omega')}{\omega'^2 - \omega^2} d\omega' \quad (6)$$

Optical absorption spectrum is used to conclude optical features of various compounds [26]. The optical properties of Fe, Mn and V doped PbSe are determined and compared with each other. The highest peaks of real part $\varepsilon_1(\omega)$ of $\text{Pb}_{1-x}\text{Fe}_x\text{Se}$, $\text{Pb}_{1-x}\text{Mn}_x\text{Se}$ and $\text{Pb}_{1-x}\text{V}_x\text{Se}$ ($x=25\%$) are 55, 35 and 66, respectively (see Fig. 6 (a)). The material also shows the metallic nature at specific energy because $\varepsilon_1(\omega)$ of the dielectric constant $\varepsilon(\omega)$ shows lowest peaks at negative value which presents that incident EM-waves are completely reflected.

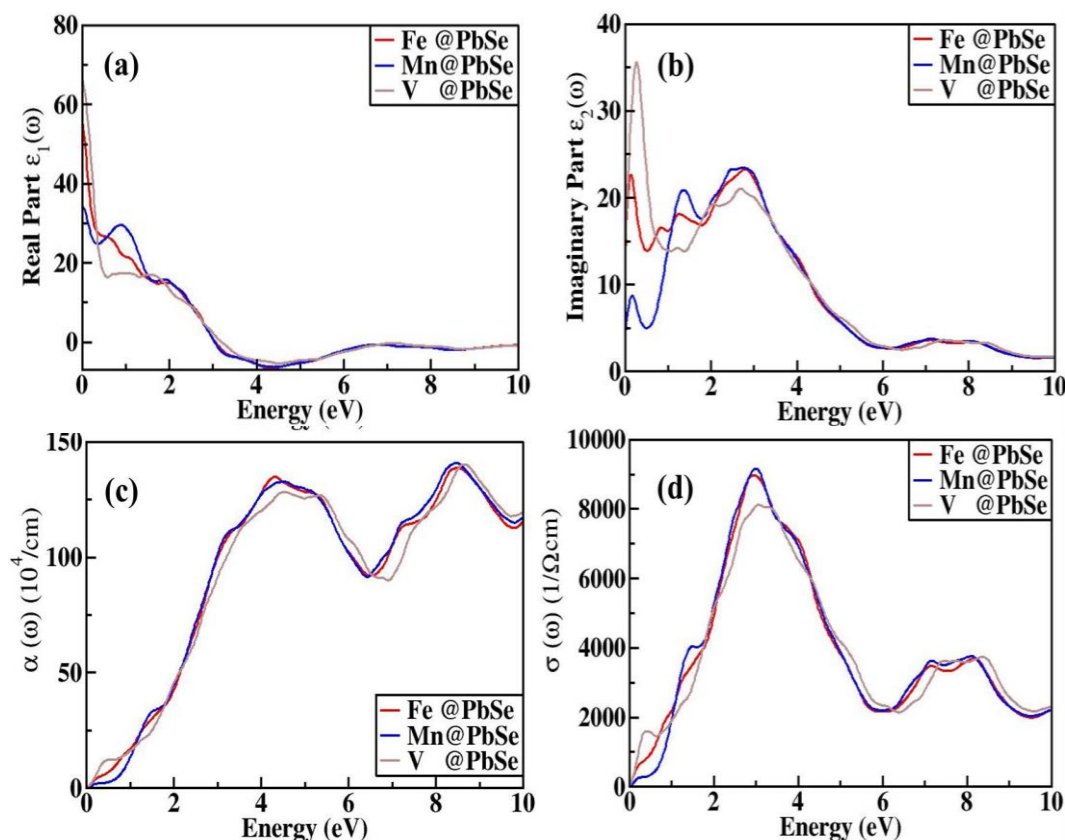


Fig. 6. (a) $\varepsilon_1(\omega)$ (b) $\varepsilon_2(\omega)$ (c) $\alpha(\omega)$ (d) $\sigma(\omega)$ of Fe, Mn and V doped PbSe.

The highest peaks of imaginary (see Fig. 6 (b)) part $\varepsilon_2(\omega)$ of Fe, Mn and V doped PbSe are appeared at 2.75, 2.68 and 0.267 eV, respectively. It can be clearly observed that $\text{Pb}_{0.75}\text{V}_{0.25}\text{Se}$ have highest peak as compared to the $\text{Pb}_{0.75}\text{Fe}_{0.25}\text{Se}$ and $\text{Pb}_{0.75}\text{Mn}_{0.25}\text{Se}$. $\alpha(\omega)$ is basically used to

determine the strength of penetration of the incident light. It depends on the absorption of interacting light (wavelength) [26]. Therefore, $\alpha(\omega)$ is examined by using the following formula:

$$I(\omega) = \frac{4\pi}{\lambda} \left(\frac{[\varepsilon_1^2(\omega) + \varepsilon_2^2(\omega)]^{\frac{1}{2}} + \varepsilon_1(\omega)}{2} \right)^{\frac{1}{2}} \quad (7)$$

The value of absorption coefficient $\alpha(\omega)$ of Fe, Mn and V doped PbSe is illustrated in Fig. 6(c). It is realized that $\alpha(\omega)$ increases with increase in energy but after 8.5 eV it starts decreasing. The maximum peaks of $\text{Pb}_{0.75}\text{Fe}_{0.25}\text{Se}$, $\text{Pb}_{0.75}\text{Mn}_{0.25}\text{Se}$ and $\text{Pb}_{0.75}\text{V}_{0.25}\text{Se}$ are appeared (see Fig. 6 (c)) at 8.45, 8.45 and 8.64 eV, respectively and at this energy range, values of $\alpha(\omega)$ are 139, 142 and 141, respectively.

$\sigma(\omega)$ is the property of material which links electric field to the current density for the common frequencies. The values of the highest peak of $\sigma(\omega)$ appeared (see Fig. 6(d)) at the 2.95, 2.97 and 3.06 eV, correspondingly. The refractive index $n(\omega)$ of Mn, V and Fe doped PbSe is plotted in Fig. 7(a) and can be computed with the given expression:

$$n(\omega) = \left(\frac{[\varepsilon_1^2(\omega) + \varepsilon_2^2(\omega)]^{\frac{1}{2}} + \varepsilon_1(\omega)}{2} \right)^{\frac{1}{2}} \quad (8)$$

The values of $n(\omega)$ are 7.5, 5.9 and 8.2 for $\text{Pb}_{0.75}\text{Fe}_{0.25}\text{Se}$, $\text{Pb}_{0.75}\text{Mn}_{0.25}\text{Se}$ and $\text{Pb}_{0.75}\text{V}_{0.25}\text{Se}$, respectively and all these values appeared at 0 eV energy. The intensity of $n(\omega)$ decreased with increase in energy which represents that when energy of incident photon increments, $n(\omega)$ decreases gradually. The $n(\omega)$ of V doped PbSe is higher as compared to Fe and Mn doped PbSe at 0 eV energy.

The $K(\omega)$ is the part of refractivity and it represents $i\varepsilon_2(\omega)$. The values of $K(\omega)$ are 3.3, 3.4 and 3.1 for $\text{Pb}_{0.75}\text{Fe}_{0.25}\text{Se}$, $\text{Pb}_{0.75}\text{Mn}_{0.25}\text{Se}$ and $\text{Pb}_{0.75}\text{V}_{0.25}\text{Se}$, respectively which appeared at 3.1, 3.1 and 3.5 eV, correspondingly (see Fig. 7(b)). At 3.1 eV the large amount of the absorption occurs so the value of $K(\omega)$ of $\text{Pb}_{0.75}\text{Mn}_{0.25}\text{Se}$ is maximum. Moreover, the $n(\omega)$ is smaller as compared absorption coefficient $\alpha(\omega)$, therefore these materials are useful for the solar cell industry.

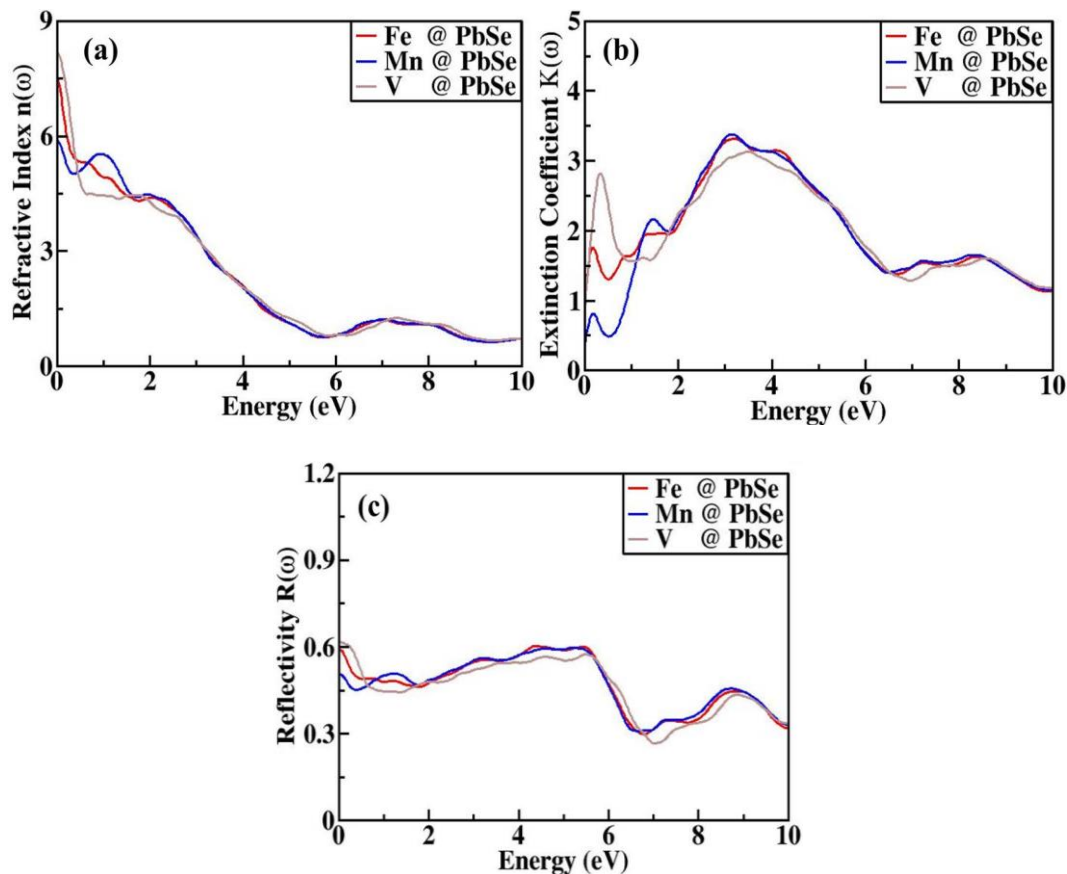


Fig. 7. (a) $n(\omega)$ (b) $K(\omega)$ (c) $R(\omega)$ of Fe, Mn and V doped PbSe.

The $R(\omega)$ of materials is the ratio of incident light and the reflected light. The $R(\omega)$ of Fe, Mn and V doped PbSe binary compound has been illustrated in the below Fig 7(c). The highest peaks of $R(\omega)$ for $\text{Pb}_{0.75}\text{Fe}_{0.25}\text{Se}$, $\text{Pb}_{0.75}\text{Mn}_{0.25}\text{Se}$, $\text{Pb}_{0.75}\text{V}_{0.25}\text{Se}$ are appeared at 4.4 eV, 5.16 eV and 5.02 eV, respectively.

4. Conclusions

In this work, physical characteristics of the Fe, Mn and V doped PbSe are evaluated by using FP-LAPW method. It can be seen from the graphs that $\text{Pb}_{0.75}\text{Fe}_{0.25}\text{Se}$, $\text{Pb}_{0.75}\text{Mn}_{0.25}\text{Se}$, $\text{Pb}_{0.75}\text{V}_{0.25}\text{Se}$ shows HMF nature, which indicates the applications of these compounds in spintronics devices. The interstitial (M_{int}) for $\text{Pb}_{0.75}\text{Fe}_{0.25}\text{Se}$, $\text{Pb}_{0.75}\text{Mn}_{0.25}\text{Se}$, $\text{Pb}_{0.75}\text{V}_{0.25}\text{Se}$ are 0.14088, 0.32354 and 0.50458, respectively and total magnetic moment of the $\text{Pb}_{0.75}\text{Fe}_{0.25}\text{Se}$, $\text{Pb}_{0.75}\text{Mn}_{0.25}\text{Se}$, $\text{Pb}_{0.75}\text{V}_{0.25}\text{Se}$ are 3.94233, 4.99108 and 2.91084 μ_{B} , respectively. Furthermore, optical properties revealed the E_{g} of 0.35, 0.23 and 0.54 eV for Fe, Mn and V, correspondingly. It is concluded from this study that doping of TM Mn is most suitable doping for spintronics devices as compare to Fe and V and also $\text{Pb}_{1-x}\text{A}_x\text{Se}$ ($\text{A}=\text{Fe}, \text{Mn}, \text{V}$) compounds are suitable for optical devices .

Acknowledgements

This work was the support of King Khalid University, the Ministry of Education, and the Kingdom of Saudi Arabia for this research through a grant (RCAMS/KKU/004/21) under the research center for advanced material science. The authors also express their gratitude to Princess

Nourah bint Abdulrahman University Researchers Supporting Project number (PNURSP2022R81), Princess Nourah bint Abdulrahman University, Riyadh, Saudi Arabia.

References

- [1] R. Sharma, S.A. Dar, A.K. Mishra, *Journal of Alloys and Compounds* 791, 983-993 (2019).
<https://doi.org/10.1016/j.jallcom.2019.03.361>
- [2] S.A. Aldaghfag, M. Yaseen, H. Ambreen, M.K. Butt, M. Rehan, A. Dahshan, *Chalcogenide Letters*, 18(7), 357-365 (2021).
- [3] SA. Sofi, S. Ahmad, S. Yousuf, DC. Gupta, *Computational Condensed Matter*, 19 (00375) (2019)
<https://doi.org/10.1016/j.cocom.2019.e00375>
- [4] SA. Sofi, S. Ahmad, DC. Gupta, *Journal of solid State Chemistry*, 284 (121178) (2020).
<https://doi.org/10.1016/j.jssc.2020.121178>
- [5] SA. Sofi, S. Ahmad, DC. Gupta, *International Journal of Energy Research*, (44), 2137-49 (2020).
<https://doi.org/10.1002/er.5071>
- [6] RA. De Groot, FM. Mueller, PG. Van Engen, KHJ. Buschow, *Physical Review Letters*, 50(25), 2024(1983).
<https://doi.org/10.1103/PhysRevLett.50.2024>
- [7] H. Itoh, T. Ohsawa, J. Inoue, *Physical Review Letters*, 84(11), 2501 (2000)
<https://doi.org/10.1103/PhysRevLett.84.2501>
- [8] K. Schwarz, *Journal of Physics F: Metal Physics*, 16(9), L211 (1986)
<https://doi.org/10.1088/0305-4608/16/9/002>
- [9] N.C. Bristowe, J. Varignon, D. Fontaine, E. Bousquet, P. Ghosez, *Nature Communications*, 6(1), 1-6(2015)
<https://doi.org/10.1038/ncomms7677>
- [10] M. Yaseen, H. Ambreen, U. Shoukat, M. Butt, S. Noreen, S. Rehman, S. RAMAY, *Journal of Ovonic Research* 15(6), 401-409 (2019).
- [11] Y. Zhang, X. Ke, C. Chen, J. Yang, P. R. C. Kent, *Physical review B*, 80(2), 024304 (2009).
<https://doi.org/10.1103/PhysRevB.80.024304>
- [12] M. Asghar Khan, Z. A. Shah, J. Khan, Y. Arifat, S. Hayat, *Journal of Theoretical and Computational Science* 4(159), 2 (2017).
- [13] M. Goano, E. Bellotti, E. Ghillino, G. Ghione, K. F. Brennan, *Journal of Applied Physics*, 88(11), 6467-6475 (2000).
<https://doi.org/10.1063/1.1309046>
- [14] L. Etgar, G. Leitus, L. Fradkin, Y. G. Assaraf, R. Tannenbaum, E. Lifshitz, *ChemPhysChem* 10(13), 2235-2241 (2009).
<https://doi.org/10.1002/cphc.200900345>
- [15] B. U. Haq, S. AlFaify, R. Ahmed, A. Laref, Q. Mahmood, E. Algrafy, *Applied Surface Science* 525, 146521 (2020).
<https://doi.org/10.1016/j.apsusc.2020.146521>
- [16] Y. Gai, H. Peng, J. Li, *The Journal of Physical Chemistry C* 113(52), 21506-21511 (2009).
<https://doi.org/10.1021/jp905868f>
- [17] S. Saleem, M. Yaseen, S.A. Aldaghfag, Misbah, R. Neffati, *Physica Scripta*,
<https://doi.org/10.1088/1402-4896/ac8a27>.
<https://doi.org/10.1088/1402-4896/ac8a27>
- [18] M.K. Butt, M. Yaseen, I. A. Bhatti, J. Iqbal, Miabah, A. Murtaza, M. Iqbal, M. M. AL-Anazy, M.H. Alhossainy, A. Laref, *Journal of Materials Research and Technology*, 9(6), 16488-16496 (2020).
<https://doi.org/10.1016/j.jmrt.2020.11.055>
- [19] G. Murtaza, N. Yousaf, A. Laref, M. Yaseen, *Zeitschrift für Naturforschung A* 73(4), 285-293 (2018).
<https://doi.org/10.1515/zna-2017-0388>
- [20] Q. Mahmood, M. Hassan, M. Yaseen, A. Laref, *Chemical Physics Letters*, 729, 11-16 (2019).
<https://doi.org/10.1016/j.cplett.2019.05.011>

- [21] M. Rashid, Z. Abbas, M. Yaseen, Q. Afzal, A. Mahmood, S.M. Ramay, *Journal of Superconductivity and Novel Magnetism*, 30(11), 3129-3136 (2017)
<https://doi.org/10.1007/s10948-017-4099-0>
- [22] N.Boukhris, H. Meradji, S. Amara Korba, S. Drablia, S. Ghemid, F. El Haj Hassan. *Bulletin of Materials Science* 37(5), 1159-1166 (2014).
<https://doi.org/10.1007/s12034-014-0057-7>
- [23] A.Paul, G. Klimeck, *Applied Physics Letters*, 98(21), 212105 (2011).
<https://doi.org/10.1063/1.3592577>
- [24] M.Yaseen, H. Ambreen, U. Shoukat, M. K. Butt, S. Noreen, S. Ur. Rehman, J. Iqbal, S. Bibi, A. Murtaza, S. M. Ramay, *Journal of Ovonic Research*, 15(6), 401-409 (2019).
- [25] P.Li, C. W.Zhang, J.Lian, M. J.Ren, P. J.Wang, X. H. Yu, S.Gao, *Optics Communications*, 295, 45-52 (2013).
<https://doi.org/10.1016/j.optcom.2012.12.086>
- [26] M.Yaseen, H.Ambreen, A.Sufyan, M.K.Butt, S. UrRehman, J.Iqbal, Misbah, S.Bibi, A. Murtaza, S.M.Ramay, *Ferroelectrics* 557(1), 112-122 (2020).